

# A Transect of 200 Shallow Shear Velocity Profiles Across the Los Angeles Basin

Weston A. Thelen,<sup>1,2,3</sup> Matthew Clark,<sup>1,4</sup> Christopher T. Lopez,<sup>2</sup> Chris Loughner,<sup>1,5</sup> Hyunmee Park,<sup>2,6</sup> James B. Scott,<sup>1</sup> Shane B. Smith,<sup>2</sup> Bob Greschke,<sup>7</sup> and John N. Louie<sup>1,2</sup>

1. Nevada Seismological Laboratory, University of Nevada MS 174, Reno, NV 89557

2. Department of Geological Sciences and Engineering, University of Nevada MS 172, Reno, NV 89557

3. Now at: Dept. of Earth and Space Sciences, University of Washington, Box 351310, Seattle, WA 98195-1310

4. Now at: U.S. Dept. of Agriculture NRS-NSL, 15 C.R. 304, Oxford, MS 38655

5. Now at: Dept. of Atmospheric and Oceanic Science, University of Maryland, College Park, MD 20742

6. Now at: Dept. of Geological Sciences, Univ. of South Carolina, 701 Sumter St. EWS 617, Columbia, SC 29208

7. IRIS-PASSCAL Instrument Center, New Mexico Tech, 100 East Road, Socorro, NM 87801

Revised for the *Bulletin of the Seismological Society of America*, Dec. 1, 2005

## Abstract

This study assesses a 60 km NNE-SSW transect along the San Gabriel River for shallow shear velocities, in San Gabriel Valley and the Los Angeles Basin of southern California. We assessed a total of 214 sites, 199 along the transect at 300 m spacing, during a one-week field campaign with the refraction microtremor (ReMi) technique. The transect's maximum 30-meter shear velocity ( $V_s^{30}$ ) occurs in coarse alluvium of San Gabriel Valley where the San Gabriel River exits the San Gabriel Mts.; at 730 m/s, upper NEHRP site class C. Much of the northeast section of the transect (in San Gabriel Valley) is also NEHRP class C, or near the CD class boundary. The section of the transect south from Whittier Narrows to Seal Beach shows NEHRP-D velocities in active alluvium. The transect's lowest  $V_s^{30}$ , 230 m/s at the Alamos Bay estuary, is also classed as NEHRP-D. An increase toward the NEHRP CD class boundary occurs at the shoreline beach outside Alamos Bay, confirmed by additional measurements on Seal Beach. Our measured  $V_s^{30}$  values generally show good correlation with published site-classification maps and existing borehole data sets. There is no evidence in our data for an increase in velocity predicted by Wills et al. (2000) at their "CD" to "BC" site classification boundary at the San Gabriel Mountains front, nor for any decrease at their "D" to "DE" class boundary at Alamos Bay. Very large  $V_s^{30}$  variations exist in soil and geologic units sampled by our survey. The  $V_s^{30}$  variations we measured are smaller than  $V_s^{30}$  variations of 30% or more we found between closely spaced (<0.5 km) downhole measurements in the Los Angeles Basin, which are not uncommon within a community data set we examined showing hundreds of boreholes. We find the San Gabriel River's hydraulic gradient to be a good predictor of minimum  $V_s^{30}$ , based on the expected effect of the hydraulic gradient on the grain size of sediments deposited by a river. The  $V_s^{30}$  data show a fractal spatial dependence, which appears at distances greater than 700 m. The unprecedented number of shear-velocity measurements we have made suggests that large measurement populations may be necessary to properly characterize  $V_s^{30}$  trends within any surficial geological unit.

## Introduction

We evaluate a 60-km-long transect for shallow shear velocities along the San Gabriel River, southern California (Fig. 1). The experiment, completed in July 2003, was designed to collect a very large number of site assessments and evaluate the spatial variability of the earthquake shaking hazard, as well as any velocity correlations to mapped geological and soil units. Shaking hazard is defined in relation to shear velocity by the National Earthquake Hazards Reduction Program (NEHRP) classification. This study was inspired by the transect of Scott et al. (2004) across the Reno, Nevada urban basin, in which 55 shear-velocity profiles were

collected using the same methods and procedures as this study. They found that 82% of their measurements were significantly higher than values predicted from geologic maps and regional hazard assessments (for example, as by Wills et al., 2000, for California).

*Background* – Shallow shear-wave velocity has proved to be an important indicator of surficial horizontal acceleration and amplification produced in varying geologic units by strong ground motions produced by earthquakes (Tinsley and Fumal, 1985; Borchardt et al., 1991; BSSC, 1998). The vertically averaged 30-meter shear velocity ( $V_s^{30}$ ) is used to determine a NEHRP soil hazard classification for

earthquake shaking as outlined by the NEHRP-UBC provisions (BSSC, 1998). The most common technique for obtaining  $V_s^{30}$  measurements is through borehole surveys. However, the high cost of these measurements has driven the search for alternative methods of estimating  $V_s^{30}$  values for NEHRP-UBC code compliance. Louie (2001) developed the *Refraction Microtremor* (ReMi) technique as such an alternative. In this method, microtremor noise from sources such as traffic on streets and freeways excites Rayleigh waves, which are recorded by a linear array of vertical refraction geophones. The resulting noise records are transformed into frequency ( $f$ ) – slowness ( $p=1/v$ ) space ( $p$ - $f$  space) as suggested by McMechan and Yedlin (1981), and a dispersion curve is picked by an analyst. Forward modeling of the fundamental-mode Rayleigh wave dispersion curve produces a depth vs. velocity sounding, which can be vertically averaged to a single  $V_s^{30}$  value required by the NEHRP-UBC code.

The ReMi method is similar to three other surface-wave measurement techniques, the microtremor-array (e.g., SPAC), the spectral analysis of surface waves (SASW), and the multichannel analysis of surface waves (MASW) techniques (Louie, 2001). Brown et al. (2002) compared SASW measurements to borehole measurements at 10 strong-motion sites in the Los Angeles area. In 7 out of 10 cases, the SASW method produced the same NEHRP classification as the borehole method. In the other three cases, the borehole method produced a  $V_s^{30}$  only 5-13 m/s above a NEHRP classification boundary. In all cases, the differences in predicted ground motion amplifications between the SASW method and the borehole method was less than 15% at most frequencies (Brown et al., 2002).

Y. Liu et al. (2004) used a combination of the ReMi method and the SASW method in Las Vegas Valley to characterize surface-wave dispersion across a wide frequency band. In all 12 of their comparisons where measurement frequencies overlapped, results of the SASW method and of the ReMi method agreed very well. H. Liu et al. (2000) compared the microtremor-array method to two borehole shear-velocity profiles in Southern California. In one case the two methods agreed to within 11%. In the other case, the two methods agreed to within 20%.

The ReMi method was initially introduced and tested by Louie (2001). Dispersion-curve picks derived from the ReMi method were compared against results of a microtremor accelerometer array installed by Iwata et al. (1998), and the dispersion curves were comparable between 1.8 and 7 Hz. Louie (2001) also compared the results of the ReMi method to the suspension log at the ROSRINE borehole in

Newhall, California, finding s-wave velocity agreement within 15% at depths to 100 m.

More recently, Martin and Diehl (2004) compared the results of several surface wave techniques, including the ReMi method, against borehole measurements at 53 sites across the Western United States, Kentucky and Russia. They found reliability of all of the surface wave methods to within 10% of borehole measurements. They concluded that surface wave techniques may characterize  $V_s^{30}$  better in areas of high geologic variability, due to the averaging nature of surface wave velocities, compared to the point measurements of borehole data. Stephenson et al. (2005) compared ReMi results to four boreholes in the Santa Clara Valley, California. When comparing the  $V_s^{30}$  values, the ReMi results were within 15% of the suspension-logger values. The calculated  $V_s^{50}$  and  $V_s^{100}$  values (averages to 50 and 100 m depths, respectively) were all within 27% of the borehole values; most were within 15%.

Explaining the variations in seismic shaking across the Los Angeles Basin has been an ongoing research topic for 20 years. Tinsley and Fumal (1985) assigned individual shear-wave velocities to each geologic unit in their testing area, taking into account age, grain size and depth. In 1994, the Northridge earthquake resulted in unexpected variations of damage and ground motions in and around the Los Angeles area. Immediately thereafter, a number of studies were launched to study ground motion effects in southern California. Park and Elrick (1998) extracted  $V_s^{30}$  measurements from boreholes to characterize deposits of different ages. Their results also show that  $V_s^{30}$  varies with grain size and age, and accordingly they grouped the geologic units in southern California into eight categories. As part of the Southern California Earthquake Center (SCEC) Phase III Report, Wills et al. (2000) published a site-conditions map for all of California based on localized field mapping, 1:250,000 scale geologic maps and 556  $V_s^{30}$  measurements statewide (Fig. 1). Wills et al. (2000) used seven categories, based on NEHRP classes, to group geologic units.

## Methods

The route for our transect was selected based on ease of access, ample “microtremor” noise and route continuity (Fig. 1). Along the 60 km transect, rolled arrays of IRIS/PASSCAL “Texan” single-channel recorders were deployed, each mated to a single 4.5-Hz vertical-component geophone. Our configuration optimizes the recording of Rayleigh waves at about 3 Hz (Satoh et al., 2001).

Linear arrays of 30 channels at a spacing of 20 m (580 m total array length) were installed for 30

minutes recording time, the same procedure used by Scott et al. (2004) for a transect in Reno, Nevada. The geophones were oriented with a bullseye level to within 10° of vertical at each channel, and recorded dominantly microtremor noise generated from heavy traffic on Interstate 605 and nearby surface streets. Employing four teams of 3 students enabled each array segment of the transect to be installed in a “chaining” fashion. To assess the spatial continuity of measured shear-velocity values, eight arrays were placed laterally to the transect, as much as 5 km away. Data collection along the complete transect with 107 array placements was completed in 4.5 days.

For our analysis, each array was divided into two 285-m segments (15 channels). Data reduction was completed using Optim’s SeisOpt® ReMi™ package, developed as part of the study by Louie (2001). This analysis produces a velocity-spectral image for each 300-m array, from which we picked a Rayleigh-wave fundamental-mode phase-velocity dispersion curve. Each curve is forward modeled to obtain a shear-velocity versus depth sounding. Each sounding was averaged to a 30-m shear velocity ( $V_s^{30}$ ), a standard used in estimating the amplification of ground motions at a given site (Borcherdt et al., 1991; BSSC, 1998).

*Sources of error-* One potential source of error in the analysis lies in our forward modeling. To minimize modeling bias in the results, three separate analysts worked on the data from the San Gabriel River transect. Each worker modeled every third sub-array throughout the length of the transect. In this way, any modeling bias of a particular worker would not characterize the results over a particular stretch of transect, especially if a certain section was geologically prone to differences in interpretation. To estimate the error introduced by forward modeling, independent modelers reanalyzed data sets from three randomly selected sites along the line (Table 1). The results show a maximum  $V_s^{30}$  difference of  $\pm 7\%$  relative to the original models.

Throughout the length of the route, shear-velocity values were measured with arrays placed upon an engineered levee between one and four meters in height above the surrounding alluvium. To assess the effect of the levee, shear-velocity measurements were made both on a ~3-m-high levee, and longitudinally adjacent to the same levee at ground level approximately 30 m away. The results show only a 4.0 m/s difference in  $V_s^{30}$  on the levee compared to off the levee, significantly less than the  $\pm 20\%$  error in velocity stated generally by Louie (2001). Inspection of the modeled shear-velocity versus depth soundings shows very little difference

between the on-levee and the off-levee measurements.

## Results

The 199 modeled shear-velocity profiles along the transect have been projected for their respective intervals onto a vertical cross section that extends to 200 m depth below the surface trace of the transect (Fig. 2). The location of interval midpoints on the surface is based on the line distance from the first recording geophone at the mouth of San Gabriel Canyon in Azusa.

Note that a “dog leg” through the Santa Fe Dam catchment area near Azusa diverts the line in a direction transverse to the San Gabriel River and results in a relatively high density of data points over the corresponding longitudinal interval of river course (Fig. 1). Likewise, the  $V_s^{30}$  averages computed for each array have been plotted as a function of transect distance in Fig. 3. The effects of off-line elevation changes are negligible in these projections.

Near the San Gabriel range front, at the mouth of San Gabriel Canyon, higher velocity materials ( $>760$  m/s) occur at depths of  $> 40$  m (Fig. 2), while  $V_s^{30}$  values cluster in the 550–660 m/s range (Fig. 3). At approximately 10 km distance south from the range front, thicker deposits of relatively low-velocity materials ( $<550$  m/s; light shades on Fig. 2) are first observed. Our highest measured velocities occur at 5–10 km from the range front in Azusa, at depths greater than 75 m. Our lowest velocities occur near the surface at approximately 56 km along the transect near Alamitos Bay (Fig. 2).

The  $V_s^{30}$  values averaged from the modeled velocity profiles for each of 199 transect arrays and 8 lateral arrays are shown graphically in Figure 3. Between Azusa and the Santa Fe Dam area (0–10 km),  $V_s^{30}$  values are in the NEHRP-C (350–760 m/s) classification. Values in this interval are more spatially variable with respect to our other measurements, than elsewhere in the transect. From the Santa Fe Dam catchment basin to north of Whittier Narrows Dam (10–37 km), values fluctuate near the NEHRP CD boundary. From Whittier Narrows south to the end of the line at Seal Beach, the modeled  $V_s^{30}$  values are classified as NEHRP-D (150–350 m/s). The spatial variability in the interval between Whittier Narrows and Seal Beach is far less, with respect to our measurements, than values north of the Whittier Narrows. The rise in  $V_s^{30}$  past Alamitos Bay toward the NEHRP CD boundary at the shore is supported by corroborating measurements at Seal Beach (Fig. 3).

To explore the relationship of  $V_s^{30}$  to surficial geology and soil type, we compared surficial units, classified by Quaternary geologic maps

(CDMG, 1998), soil maps (NRCS, 1969), and the Wills et al. (2000) predicted hazard classes against the distribution of  $V_s^{30}$  over our transect. Each midpoint of a 300-m sub-array was associated by hand with a geologic unit, soil type, and hazard class. The measured  $V_s^{30}$  values are plotted against geologic unit, soil type, and predicted hazard class from Wills et al. (2000), in Figures 4, 5, and 6, respectively. Refer to Tables 2 and 3, respectively, for descriptions of each of the geologic and soil units.

## Discussion

*Velocity section*— Shear-velocity trends in the velocity cross-section (Fig. 2) are consistent with velocities predictable from basic sedimentological concepts of river energy and river gradient (Tarbuck and Lutgens, 1996). For example, near the mouth of San Gabriel Canyon, high velocities ( $\geq 800$  m/s) come to within 40 m of the surface, suggesting either thick sequences of well-graded large clasts, such as boulders or cobbles, or very weak and fractured rock below that depth. Magistrale et al. (2000) expect a deep ( $>1700$  m) basin underlies Azusa, so bedrock is unlikely in the upper 200 m of the section south of San Gabriel Canyon. At  $\sim 10$  km from the range front, the high velocities show an abrupt deepening, suggesting a change from very coarse, alluvial fan-type detritus to finer grained-distal alluvial material. Likewise, the thickness of low-velocity material increases with distance from the range front, probably reflecting the increasing fraction of smaller grains, such as sands and silts as the San Gabriel River's stream energy decreases, losing its ability to carry coarser-grained material.

*Comparison with Wills et al. (2000) predictions*— In order to facilitate the discussion of our results, we compare our  $V_s^{30}$  results to the predictions of Wills et al. (2000) in Figure 3 and Figure 6. Within the San Gabriel Mountains north of the range front (0-2 km, Figs. 2 & 3), our  $V_s^{30}$  measurements reveal NEHRP-C velocities, at the low end of the predicted range of the Wills et al. (2000) "BC" class. The slightly lower than expected  $V_s^{30}$  values are likely due to the pervasive fracturing and a thick weathered zone that has crumbled and reduced the intact rock and increased the porosity. Local variability in fracture density and the presence of a veneer of coarse-grained alluvium and colluvium likely also contribute to our measured  $V_s^{30}$  values being lower than predicted.

From Azusa to the Santa Fe Dam area (2-10 km, Figs. 2 & 3) the measured  $V_s^{30}$  values are higher than those predicted by Wills et al. (2000). This is probably due to the presence of coarser deposits of boulders and cobbles at shallow depths, in contrast to the finer-grained sediment classes applied to this area

by the geological and hazard maps. Such bouldery alluvium was also not well sampled by the boreholes used in Wills et al. (2000), so is not surprising that many new measurements of a unit would shift the average  $V_s^{30}$  values.

From Santa Fe Dam south to near El Monte (15-30 km, Figs. 2 & 3), our modeled velocities are higher than predicted, again possibly due to coarse-grained lenses at shallow depths. Coarse-grained lenses of cobbles and gravels may have been widely deposited across this portion of the transect as the course of the San Gabriel River channel migrated during Quaternary times across its alluvial fan in San Gabriel Valley. Coarse-grained deposits might also be expected with the higher volumetric discharges characteristic of past pluvial periods.

From Whittier Narrows to the terminus of our line at Seal Beach (30-60 km, Figs. 2 & 3), almost all of the measured  $V_s^{30}$  values are in agreement with the site-conditions map of Wills et al. (2000). It should be noted that our measurements show no difference in velocities across the classification boundaries north and south of Alamitos Bay that Wills et al. (2000) predicted would fall from class D to class DE (55-57 km, Figs. 2 & 3).

For a dominant portion of the transect, the  $V_s^{30}$  values are near the upper ends of the CD and D ranges predicted by Wills et al. (2000; Figs. 3 & 6 here). The measured  $V_s^{30}$  values for the northern 17 km of the transect fall within the NEHRP-C classification (350-760 m/s) rather than within the BC or CD classifications assigned by Wills, et al. (2000) for this interval. Our measurements at Alamitos Bay barely fall to the upper boundary of their DE classification (for  $V_s^{30}$  of 90-270 m/s; Fig. 3), predicted for Alamitos Bay north of Seal Beach (Figs. 1 & 3).

*Comparison to borehole data sets*— Borehole data sets measured by Gibbs et al. (2000) and Gibbs et al. (2001) include sites near our transect. A community data set assembled by Wills and Silva (1998) and by Wills et al. (2000; with later updates from C. Wills, pers. comm., 2005) cover the Los Angeles and San Gabriel Valley basins. In these data sets, 4 boreholes were present within 1 km of our transect. One additional nearby borehole logged by the ROSRINE project can be found at [geoinfo.usc.edu/rosrine](http://geoinfo.usc.edu/rosrine) in Pico Rivera 221 m from our transect. (The next closest ROSRINE log is at Downey South Middle School, 2.4 km from our transect.) A comparison of summary  $V_s^{30}$  values for each of these boreholes with nearby measurements in our transect is shown in Table 4. In four out of the five cases at less than 1 km distance, our closest measurement agrees with the NEHRP classification derived from the borehole measurement. In three out

of five of those cases, the  $V_s^{30}$  values agree within 15%.

The variability of our  $V_s^{30}$  values is to be expected since our measurements do not co-locate with the sites of the borehole measurements. None of our array centers were less than 221 m from a borehole, nor did any arrays pass over any borehole site. Stephenson et al. (2005) located measurement arrays within meters of boreholes in northern California and still found significant variability, in blind comparisons of various surface techniques including ReMi against suspension-logger results.

In Figure 7, we explore the internal variability of our ReMi and the existing Los Angeles borehole data sets as a function of distance between measurements. We use the natural logarithm of the ratio of the  $V_s^{30}$  values as a proxy for variability. We make separate comparisons of the internal spatial variability of our ReMi  $V_s^{30}$  data set (Fig. 7a), and of the internal variability of the borehole  $V_s^{30}$  data set for the Los Angeles Basin (Fig. 7b). The boreholes selected for that data set include five sites from Gibbs et al. (2000) and twelve from Gibbs et al. (2001), added to 243 sites from a data set compiled by Wills and Silva (1998) and updated to April 2005 (C. Wills, pers. comm., 2005). All of the sites we used from the data set are in or near the Los Angeles and San Gabriel Valley basins.

For both data sets, the variability increases with distance and variability exists even when the distances are very small (Fig. 7c,d). In general, our ReMi measurement set shows less internal variability with distance, with a maximum ratio between measurements of 3.3 (with a natural log of 1.2 on Fig. 7a) appearing at >30 km distance. The borehole data set, on the other hand, shows ratios over a factor of 5 ( $\ln=1.6$  on Fig. 7d) at distances as small as 2 km. The lower variability of our data set could be the combined effect of the limited range of site classes our transect sampled, together with the spatial averaging over 300-m-long arrays inherent to the ReMi technique (Louie, 2001). The point-measurement nature of downhole or suspension-logger measurements in a bore may increase the variability of borehole velocity results.

One example of the spatial variability of borehole data comes from Gibbs et al. (2000). Downhole measurements at the Sylmar Converter East and the Sylmar Converter East #2 boreholes were only separated by 253 m. These measurements were in northern San Fernando Valley (thus not included in the analysis of Fig. 7) in silty alluvium with gravel lenses similar to what our transect crossed in Pico Rivera. The two measurements yielded  $V_s^{30}$  values of 371 m/s and 281 m/s respectively. Despite their close proximity, the  $V_s^{30}$

values differ by 32%. The natural log of their  $V_s^{30}$  ratio is 0.28, comparable to points on Fig. 7d at 0.3 km. Another example comes from Wills and Silva (1998). The downhole measurement at the Cedar Hills Nursery in Tarzana and the ROSRINE Tarzana suspension log are separated by 144 m. These measurements were in Tertiary shale. They yielded  $V_s^{30}$  values of 380 m/s and 257 m/s respectively, differing by 48%. The natural log of their  $V_s^{30}$  ratio is 0.39.

The one case in Table 4 where our measurements did not agree with the NEHRP classification of a nearby borehole is detailed in Figure 8. This figure shows that our closest transect ReMi profiles match the ROSRINE Pico Rivera 2 log well below 8 m depth. Array number 154A at a transect distance of 31.8 km (Figs. 2 & 3) provides the best match. The modeled velocity increase from 233 m/s to 463 m/s at 10.5 m depth mimics well a similar sharp shear-velocity increase in the suspension log.

Above 8 m depth, the ROSRINE borehole encountered very slow materials, probably soft and partly-saturated clays. (The borehole's P-velocity log suggests an 8-m depth for the water table.) There is no documentation at Rosrine of the quality of the suspension-logger measurements in this hole, so the reliability of the slow values reported above the water table is not known. The measurements below the water table are quite reasonable.

Our measurements were all completed on an engineered levee, closer to coarser materials in the active river channel, and where the soft materials may have been removed or modified during levee construction. While the closest ReMi array 154A yielded a  $V_s^{30}$  of 381 m/s, the very soft 100-200 m/s materials logged above 8 m give the ROSRINE result a slowness-averaged  $V_s^{30}$  of only 242 m/s. Figure 3 does show that one ReMi array 1.5 km to the south of the ROSRINE borehole, at 35 km transect distance, yielded a  $V_s^{30}$  below 300 m/s. All of these ReMi measurements were a close match instead to the nearby Lakeview School, Santa Fe Springs borehole, attributed to "Lin & Stokoe, personal communication (26 March 2003)," and included in the 2005 update to the Wills and Silva (1998) data set (Table 4). The difference between these closely-located boreholes is one of the manifestations of the high internal variability of the borehole dataset seen in Figure 7.

The ROSRINE Pico Rivera 2 log appears to have been performed in a USGS bore completed by J. Tinsley in a water-well production field outside the levee barriers and 221 m across the San Gabriel River from the center of our array 154A. Inspection shows this area to be completely built up. Since drilling or geotechnical log information have not been published

or posted on the ROSRINE web site as of November 2005, we cannot verify whether the slow materials logged in the upper 8 m of the bore are similar to or different from the materials in and below the engineered levee underneath our ReMi arrays.

Table 4 shows the next closest ROSRINE borehole to our transect for comparison. The USGS South Downey Middle School bore (also with a drill log not yet available) is exceptionally deep, suspension-logged to 354 m, and 2.4 km from our nearest transect measurement. We compute a  $V_s^{30}$  of 246 m/s from the ROSRINE log, close to the Pico Rivera 2 value. However, Table 4 shows that our nearest array, 164, yielded a  $V_s^{30}$  of 326 m/s, only 33% higher. As can be seen in Figure 7d, 60% differences in  $V_s^{30}$  (natural log  $V_s^{30}$  ratio of 0.5) exist within the borehole data set at 200-m distances. Such differences also appear within our ReMi measurement set at distances of 2 km (Fig. 7c).

*Measurements away from the River channel*— In order to test the spatial continuity of our transect results, corroborating measurements were taken along lines perpendicular to our transect, up to 5 km laterally distant from the riverside transect. The locations of the lateral measurements are projected back upon the line and plotted together with the transect values on Figure 3. Our lateral  $V_s^{30}$  measurements agree very well with our transect values in all but one case, suggesting less spatial variability with increasing distance from the San Gabriel range front (Fig. 3). The corroboration also suggests that we are not getting unique  $V_s^{30}$  values due to our measuring alongside the active river channel on an engineered levee. Our riverside measurements should be indicative of  $V_s^{30}$  values and variances away from the river, as well, at least to the degree suggested by the spatial analysis of Figure 7.

The the lateral measurement most different from those on the transect nearby occurs near the range front, where a highly variable geologic history characterizes the longitudinal  $V_s^{30}$  profile. A few kilometers to the east of the transect in Azusa,  $V_s^{30}$  values are approximately 160-180 m/s less than those taken on the transect beside the active channel of the San Gabriel River (Fig. 3). At that location, the  $V_s^{30}$  measurements were made in inactive older alluvium having a well developed soil, on a terrace probably tectonically elevated above the modern riverbed. We attribute this heterogeneity observed near the range front to abrupt facies changes within the surficial deposits and abrupt lateral changes in deposit ages and burial histories (and hence weathering and lithification). In the case of the uplifted Azusa terrace, shear wave velocities suggest a finer-grained deposit that was never buried, with long-term weathering and Pleistocene soil development.

*Hydraulic gradient*— Interestingly, the shape of the  $V_s^{30}$  curve (Fig. 3) loosely mimics the modern hydraulic-elevation profile of the San Gabriel River from the range-front river mouth at 0 km transect distance to its estuarine terminus at 58 km. This similarity is most likely due to the ability of a river to carry larger clasts at larger hydraulic gradients and smaller clasts at lesser gradients (Tarbuck and Lutgens, 1996). This observation is quantified by the scattergram in Figure 9. We computed a smoothed elevation gradient along the transect by matching our GPS horizontal locations of ReMi array endpoints with elevations from USGS 30-m digital elevation models. Then we smoothed the elevations with a 1.2-km-wide centered moving window (including 5 array centers) before computing the gradient.

Our smoothed gradient is an approximation of the river's original gradient. The river is now bounded by an engineered levee, and the modified channel is interrupted by hundreds of weirs up to 3 m high. The excavated, relatively flat Santa Fe Dam catchment area in the upper reaches of the river (Fig. 1) created artificially small gradients in a region where the river originally flowed at a large gradient, since the excavation is represented on the DEMs.

The  $V_s^{30}$  values in Figure 9 obviously increase correlative with an increase in hydraulic gradient. Furthermore, where the hydraulic gradient is large, the variability in measured  $V_s^{30}$  is large. This is especially obvious when comparing the variability in  $V_s^{30}$  values between 0% and 0.5% gradient, to the variability in  $V_s^{30}$  values between 0.5% and 2% gradient (Fig. 9). High variability is likely a product of discontinuous and heterogeneous fanglomerate bodies deposited proximal to the tectonically active range front of the San Gabriel Mountains during Quaternary times. The low variability we interpret to reflect an increased fraction of smaller grain sizes (i.e. sands or silts) and a greater lateral continuity of deposits near the surface. Both changes are concomitant with the change to an alluvial and fluvial setting more distal from sediment sources in San Gabriel Canyon (Fig. 1).

*Velocity correlations with map units*— Comparisons of  $V_s^{30}$  values measured within mapped Quaternary geologic and soil units reveal high variability in most instances. Large ranges of up to  $\pm 150$  m/s are observed in ten out of the eleven Quaternary geologic units encountered in the transect (Fig. 4). In many cases, variations within units are larger than the differences in average  $V_s^{30}$  observed between different units (Fig. 4). Variability and standard deviation of  $V_s^{30}$  tend to increase as the number of measurements of a unit increases. The variances are similar to those we measured on the CD and D classes of Wills et al. (2000) shown in Figure

6. However, the differences among the  $V_s^{30}$  averages we assessed for the geologic units on Figure 4 are much smaller than the differences among unit averages on Figure 6.

It is worthy of note that in designating surficial units, Quaternary mappers may “lump” several sedimentary deposit types. Such characterizations may be based upon surface and morphologic expression in aerial photographs rather than deposit texture, lithification, or thickness. Hence mapped units may be poor predictors of the elastic properties of the units for depths exceeding several meters. In addition, the criteria for unit designations are somewhat subjective and may vary from worker to worker. Wills et al. (2000) recognized this and further lumped surficial geologic units together.

Further, our measurements do not show a correlation between  $V_s^{30}$  and river-deposit age. Figure 4 is plotted in order of the age of the Quaternary deposit with the oldest deposits on the left and the youngest deposits on the right. Traditionally, geologic units are thought to have higher  $V_s^{30}$  values as they age. In a gross sense, for instance, intact Tertiary deposits will have higher  $V_s^{30}$  values than unconsolidated Quaternary deposits. However, within Quaternary-age deposits, our data show  $V_s^{30}$  values stay the same or slightly increase with respect to decreasing river-deposit ages (Fig. 4). Wills et al. (2000) lumped geologic units of similar ages together in their classification scheme, and geologic age generally increases from their class DE to their class BC. But our results reveal that the Quaternary fluvial and alluvial geologic units lumped into their CD, D, and DE classes do not have detectable  $V_s^{30}$  trends with age.

Four of the eight soil types occurring in the transect show very high  $V_s^{30}$  variations within their respective unit (Fig. 5). These include the units with the highest populations of measurements. While we would like to find existing maps that can characterize shear velocities, it is helpful to note that the development of soil is controlled by a number of factors including slope, climate, parent material, biologic activity, and flux of aeolian silt. In addition, the degree of soil development is strongly related to length of deposit exposure at the surface ( $10^4$ - $10^6$  year scale). In tectonically active areas, some surfaces have convoluted soil-developmental histories caused by alternating periods of active sedimentation and subsequent abandonment. Because soils in the southwestern United States typically extend no more than 2 meters below the ground surface (~7% of 30 m depth), the degree to which soil development can be considered a strict indicator of the elastic properties of the deposit over a 30 m interval may be severely limited. Moreover, soil-

forming processes such as biologic activity and aeolian silt influx essentially act at the surface and thus have negligible influence over a 30-m-deep interval.

Our data do not adequately sample most soil units, so we cannot determine whether a correlation between  $V_s^{30}$  and soil unit exists. The three soil types showing a relatively low variance of  $V_s^{30}$  values within the unit may instead be indicating the subsections of the hydraulic gradient over which  $V_s^{30}$  shows homogeneity regardless of soil type. Note also that slope controls the distribution of clay minerals in the basin, which are key in the designation of mappable soil units. Further, slope also controls texture which in turn affects porosity and ultimately the thickness and type of soil formed. Thus it is only to the extent that soils are predictors of hydraulic gradient that they may be considered rough predictors of  $V_s^{30}$ .

Because the entire length of the line follows the course of the San Gabriel River, the measurements were predominantly taken on soil types 3 and 4 (Fig. 5), which are formed on top of fluvial surficial map units. Hence it may be argued that the lack of correlation between our  $V_s^{30}$  values and mapped soil and geologic units is an artifact of the transect location. This argument would predict low  $V_s^{30}$  values over our transect because the shear-wave velocity measurements are taken in relatively young and uncompacted fluvial deposits. However, our  $V_s^{30}$  measurements throughout the northern half of the transect are higher than those predicted by Wills et al. (2000). We infer that the most recent, active alluvium is coarser grained, better graded, and thus stiffer than less active parts of the sequence.

*Spatial statistics*— To further examine the relationship between our measured  $V_s^{30}$  values and the mapped geologic units, the fractal dimension of the spatial variation of  $V_s^{30}$  in Figure 3 was calculated. The power spectrum and fractal dimension, when applied to seismic data, can be related to correlation lengths of lithologic variation (Mela and Louie, 2001). We derive the fractal dimension of transect  $V_s^{30}$ s from the spatial power spectrum of the transect's  $V_s^{30}$  spatial curve (Fig. 3). The transect  $V_s^{30}$  power spectrum (Fig. 10) exhibits fractal characteristics, a linear slope down in the log-log plot. Calculated from the trend line, the fractal dimension  $D$  of 1.70 is similar to that of other spatial measurements of geologic deposits (Carr, 1995; Mela and Louie, 2001). The fractal dimension, a normal value for geologic deposits and other natural phenomena, suggests the confusing relationship between soil units, geologic units, and their  $V_s^{30}$  values seen in Figures 4 and 5 is real and not an effect of measurement or modeling errors or biases.

There is an apparent flattening of the power spectrum near 700 m separation in Figure 10, which is the noise variance level; the short spacings where our data distinguish lateral  $V_s^{30}$  variations less accurately.

Further tests of jackknifing subsampled  $V_s^{30}$  averages and standard deviations give insights into spatial dependence and variations of velocities. The best-sampled soil unit, 4, and geologic unit, Qwa, were extracted to calculate the average and standard deviation of  $V_s^{30}$  values for each 25% of the population, 50% of the population and 100% of the population. The partitioning of the data was based on measurement location, i.e., one of the 25% portions was from the southernmost 25% of the transect, another 25% portion was from the northernmost 25% of the transect, etc. Next, the  $V_s^{30}$  data for these units were randomized in location and evaluated against the spatially sorted data. In all cases, the maximum variability occurs at 25% of the population, suggesting a high degree of spatial dependence of the final shear-velocity values.

In geologic unit Qwa and soil unit 4, the randomly sorted data show much the same behavior as the spatially sorted data, with less variation. In our two highest populations, the soil variability between sections partitioned from different locations along the transect is much higher than the geologic or soil variability. In both cases, our 100% completeness average is an entirely different NEHRP classification than the lowest-velocity 25% and 50% completeness averages.

The subsampled standard deviation of soil unit 4 increases at nearly all completeness values, due to the inadequacy of soil type as a  $V_s^{30}$  indicator. This is intuitively opposite to the behavior of geologically related data, where standard deviations decrease with increasing population. The randomly sorted data show behavior that is much more indicative of geologically related data. For geological unit Qwa, the standard deviations increase with increasing completeness in 3 out of 4 cases. The randomly sorted data show the same behavior as the spatially sorted data. Further investigations are needed to explore the cause of these behaviors. The magnitudes of the increases in standard deviation are much higher for the soil unit than for the geologic unit, suggesting that the geologic unit may be a better indicator of  $V_s^{30}$ .

## Conclusions

This study has measured shear-velocity profiles at more than 200 individual sites along a 60 km transect from San Gabriel Canyon south to Seal Beach. All 99 transect arrays and eight cross-lines took only 4.5 days to complete. The modeled

velocities have depth constraints to no less than 100 m and often as deep as 300 m.

Our derived  $V_s^{30}$  values agree well with published site-conditions maps. Individual site analyses show high degrees of natural, fractal variability for separations greater than 700 m. No evidence for increases in velocity between the CD and BC hazard classes, or between the DE and the D classes of Wills et al. (2000) were found along the transect, despite many measurements across each boundary. Our values also compare well to nearby borehole results. Variability between our measurements and the borehole measurements is to be expected based on empirical comparisons within the ReMi and the borehole measurement data sets. Our examination of a data set of hundreds of downhole  $V_s^{30}$  measurements within the Los Angeles Basin reveals many instances where adjacent bores, separated by <0.5 km, provided  $V_s^{30}$  values differing by 30% or more.

Our measurements suggest the best surface indicator of  $V_s^{30}$  may be the hydraulic gradient of the San Gabriel River. Presumably, this is due to the ability of the river to deposit large clasts where the hydraulic gradient is high, and smaller grains where the hydraulic gradient is low. Near the San Gabriel River, Quaternary geologic units show no river deposit-age correlation to the measured  $V_s^{30}$ . We further find substantial  $V_s^{30}$  variance within geologic and soil units. The variance remains large regardless of how well-sampled the a unit is.

## Acknowledgements

This study was funded by the USGS NEHRP Southern California Panel under contract #03HQGR006D for \$52,000. The instruments used in the field program were provided by the PASSCAL facility of the Incorporated Research Institutions for Seismology (IRIS) through the PASSCAL Instrument Center at New Mexico Tech. Data collected during this experiment will be available through the IRIS Data Management Center. The facilities of the IRIS Consortium are supported by the National Science Foundation under Cooperative Agreement EAR-0004370 and by the Department of Energy National Nuclear Security Administration. The authors would like to thank the personnel who assisted in collecting the field data, including Warren Dang, Stephan Beck, Michael Lee and Adam Hemsley. We thank as well the City of Long Beach, the County of Los Angeles and the Army Corps of Engineers for granting encroachment permits. Chris Wills and Walt Silva kindly made an April 2005 version of their proprietary borehole  $V_s^{30}$  database available for our statistical analysis. John G. Anderson made valuable suggestions for revising the manuscript.

All data and results from this work are available from the web site [www.seismo.unr.edu/hazsurv](http://www.seismo.unr.edu/hazsurv).

## References

- Borcherdt, R. D., Wentworth, C. M., Janssen, A., Fumal, T., and Gibbs, J., 1991. Methodology for predictive GIS mapping of special study zones for strong ground motion in the San Francisco Bay region, CA, in *Proc. Fourth Int. Cont. on Seismic Zonation*, Earthquake Engineering Research Institute, Oakland, California, 545-552.
- Brown, L. T., Boore, D. M., and Stokoe II, K. H., 2002. Comparison of shear-wave slowness profiles at 10 strong-motion sites from noninvasive SASW measurements and measurements made in boreholes, *Bull. Seism. Soc. Amer.*, **92**, 3116-3133.
- BSSC: Building Seismic Safety Council, 1998. *NEHRP Recommended Provisions for Seismic Regulation for New Buildings, FEMA 302/303*, developed for the Federal Emergency Management Agency, Washington, D. C.
- Carr, J. R., 1995. *Numerical analysis for the geological sciences*, Prentice-Hall, Engelwood Cliffs, New Jersey, 592 pp.
- CDMG: California Division of Mines and Geology, 1998. Seismic hazard evaluation of the Azusa 7.5-Minute Quadrangle, Los Angeles County, California, *Open-File Report*, **98-12**, 55 pp.
- CDMG: California Division of Mines and Geology, 1998. Seismic hazard evaluation of the Baldwin Park 7.5-Minute Quadrangle, Los Angeles County, California, *Open-File Report*, **98-13**, 48 pp.
- CDMG: California Division of Mines and Geology, 1998. Seismic hazard evaluation of the El Monte 7.5-Minute Quadrangle, Los Angeles County, California, *Open-File Report*, **98-15**, 50 pp.
- CDMG: California Division of Mines and Geology, 1998. Seismic hazard evaluation of the Long Beach 7.5-Minute Quadrangle, Los Angeles County, California, *Open-File Report*, **98-19**, 52 pp.
- CDMG: California Division of Mines and Geology, 1998. Seismic hazard evaluation of the Los Alamitos 7.5-Minute Quadrangle, Los Angeles and Orange Counties, California, *Open-File Report*, **98-10**, 37 pp.
- CDMG: California Division of Mines and Geology, 1998. Seismic hazard evaluation of the Mt. Wilson 7.5-Minute Quadrangle, Los Angeles County, California, *Open-File Report*, **98-21**, 50 pp.
- CDMG: California Division of Mines and Geology, 1998. Seismic hazard evaluation of the Seal Beach 7.5-Minute Quadrangle, Los Angeles and Orange Counties, California, *Open-File Report*, **98-11**, 50 pp.
- CDMG: California Division of Mines and Geology, 1998. Seismic hazard evaluation of the Whittier 7.5-Minute Quadrangle, Los Angeles and Orange Counties, California, *Open-File Report*, **98-28**, 51 pp.
- Gibbs, J. F., Tinsley, J. C., Boore, D. M., Joyner, W.B., 2000. Borehole velocity measurements and geological conditions at thirteen sites in the Los Angeles, California region, *U.S. Geol. Surv. Open-File Rept.* **OF 00-470**, 118 pp.
- Gibbs, J. F., Boore, D. M., Tinsley, J. C., Mueller, C. S., 2001. Borehole P- and S-wave velocity at thirteen stations in southern California, *U.S. Geol. Surv. Open-File Rept.* **OF 01-506**, 117 pp.
- Iwata, T., Kawase, H., Satoh, T., Kakehi, Y., Irikura, K., Louie, J. N., Abbott, R. E., Anderson, J. G., 1998. Array microtremor measurements at Reno, Nevada, USA (abstract), *EOS Trans. AGU*, **79**, no. 45, p. F578.
- Liu, H. P., Boore, D. M., Joyner, W. B., Oppenheimer, D. H., Warrick, R. E., Zhang, W., Hamilton, J. C., and Brown, L. T., 2000. Comparison of phase velocities from array measurements of Rayleigh waves associated with microtremor and results calculated from borehole shear-wave velocity profiles, *Bull. Seism. Soc. Am.*, **90**, 666-678.
- Liu, Y., Luke, B., Pullammanappallil, S., Louie, J., and Bay, J., 2005. Combining active- and passive-source measurements to profile shear wave velocities for seismic microzonation, *Proceedings of the Geo-Frontiers 2005 Congress*, Austin, Texas, Jan. 24-26, 14 pp.
- Louie, J. N., 2001. Faster, better: Shear-wave velocity to 100 meters depth from refraction microtremor arrays, *Bull. Seism. Soc. Am.*, **91**, 347-364.
- Magistrale, H., S. Day, R.W. Clayton, and R. Graves, 2000. The SCEC Southern California reference three-dimensional seismic velocity model version 2, *Bull. Seism. Soc. Am.* **90**, no. 6B (Dec.), S65-S76. (Data available from <http://www.scec.org:8081/examples/servlet/BasicDepthServlet>)
- Martin, A. J., Diehl, J. G., 2004. Practical experience using a simplified procedure to measure average shear-wave velocity to a depth of 30 meters ( $V_s^{30}$ ), *13<sup>th</sup> World Conference on Earthquake Engineering*, paper no. **952**, 9 pp.

- Mela, K. and Louie, J. N., 2001. Correlation length and fractal dimension interpretation from seismic data using variograms and power spectra, *Geophysics*, **66**, 1372-1378.
- McMechan, G. A., and Yedlin, M. J., 1981. Analysis of dispersive waves by wave field transformation, *Geophysics*, **46**, 869-874.
- NRCS: U. S. Department of Agriculture Natural Resources Conservation Service, 1969. *Report and General Soil Map, Los Angeles County California*, 70 pp.
- Park, S., and Elrick, S., 1998. Predictions of shear-wave velocities in southern California using surface geology, *Bull. Seism. Soc. Am.*, **88**, 677-685.
- Satoh, T., Kawase, H. and Matsushima, S., 2001. Differences between site characteristics obtained from microtremors, S-waves, P-waves, and codas, *Bull. Seism. Soc. Am.*, **91**, 313-334.
- Scott, J. B., Clark, M., Rennie, T., Pancha, A., Park, H. and Louie, J. N., 2004. A shallow shear-velocity transect across the Reno, Nevada area basin. *Bull. Seism. Soc. Am.*, **94**, no. 6 (Dec.), 2222-2228.
- Stephenson, W.J., Louie, J.N., Pullammanappallil, S., Williams, R.A., and Odum, J.K., 2005. Blind shear-wave velocity comparison of ReMi and MASW results with boreholes to 200 m in Santa Clara Valley: Implications for earthquake ground motion assessment: *Bull. Seism. Soc. Am.*, **95**, no. 6, 2506–2516,
- Tarback, E. J., and Lutgens, F. K., 1996. *Earth: An Introduction to Physical Geology*, Fifth edition, Prentice Hall, Upper Saddle River, New Jersey, 605 pp.
- Tinsley, J. C., and Fumal, T. E., 1985. Mapping Quaternary sedimentary deposits for areal variations in shaking response, in *Evaluating Earthquake Hazards in the Los Angeles Region—An Earth Science Perspective*, Ziony, J. I. (Editor), *U. S. Geol. Surv. Profess. Pap.* **1360**, 101-126.
- Wills, C. J., Petersen, M., Bryant, W. A., Reichle, M., Saucedo, G. J., Tan, S., Taylor, G., and Treiman, J., 2000. A site conditions map for California based on geology and shear-wave velocity, *Bull. Seism. Soc. Am.*, **90**, no. 6B (Dec.), S187-S208.
- Wills, C. J., Silva, W., 1998. Shear wave velocity characteristics of geologic units in California, *Earthquake Spectra*, **14**, 533-556.

Distance	Nearest City	V <sub>30</sub> Values (Orig., Remodeled)	V <sub>30</sub> Average	Standard Deviation ( $\sigma$ )	$\sigma$ / V <sub>30</sub> Ave.	Approx. Diff. $\pm$ %
0.6	Azusa	584, 565	574.5	13.44	2.34%	1.17%
33.6	Whittier	347, 327	337.0	14.14	4.20%	2.10%
58.2	Seal Beach	307, 251	279.0	39.60	14.19%	7.10%

**Table 1**

<b>Symbol</b>	<b>Description</b>
Qfb	Active alluvial fan deposits, boulder gravel
af	Artificial fills, sand to silty sand, soft to dense, high liquefaction susceptibility
Qwg	Active alluvial fan deposits, active wash, gravel
Qwa	Active alluvial fan deposits, active wash
Qya4a	Young (Holocene?) alluvial valley deposits, arenaceous sand, characteristic grain size: 4a
Qyf3a	Young (Holocene?) alluvial valley deposits, arenaceous sand, characteristic grain size: 3a
Qya4g	Young (Holocene?) alluvial valley deposits, gravel, characteristic grain size: 3a
Qyfa	Younger alluvium, soft sand, loose to moderately dense sand, high liquefaction susceptibility
Qyfs	Younger alluvium, silt, loose to moderately dense, high liquefaction susceptibility
Qoaa	Old (Pleistocene?) alluvial valley deposits, silty sand, minor gravel, dense to very dense, low liquefaction susceptibility

Source: CDMG, 1998.

**Table 2**

Soil Unit Number	Description
1	<b>Oceano</b> association, over 60 inches deep, 2 to 5 percent slopes, sands, excessively drained
2	<b>Marina-Garey</b> association, over 60 inches deep, 2 to 15 percent slopes, loamy sand to sandy loam, well to excessively drained
3	<b>Tujunga-Soboba</b> association, over 60 inches deep, 0 to 5 percent slopes, sand or loamy fine sand with up to 35% gravel and cobbles, excessively drained
4	<b>Hanford</b> association, over 60 inches deep, 2 to 5 percent slopes, coarse sandy loam to gravelly loamy coarse sand with courser lenses below 40 inches, well drained
5	<b>Chino</b> association, over 60 inches deep, nearly flat slopes, loam to silt loam to clay loam to silty clay loam, poorly drained
6	<b>Ramona-Placentia</b> association, over 60 inches deep, 9 to 15 percent slopes, loam to sandy loam to clay loam, excessively drained
7	<b>Vista-Amargosa</b> association, 14 to 38 inches deep, 30 to 50 percent slopes, sandy loam, well to excessively drained
8	<b>Rock land- Rough broken land</b> association, very shallow, very flat, rock outcrops, excessively drained

Source: NRCS, 2002.

**Table 3**

<b>Borehole Data Set Comparison— Boreholes within 1 km of Transect, plus one</b>				
Source	Distance from Borehole	30-m Shear Velocity	% Diff.	NEHRP Class
<b>Gibbs et al. (2000): WTP</b>	-----	<b>226.9 m/s</b>	-----	<b>D</b>
This study, 186	850 m	309 m/s	36.18%	D
This study, 187	269 m	301 m/s	32.66%	D
This study, 188	345 m	284 m/s	25.17%	D
This study, 189	930 m	251 m/s	10.62%	D
<b>Gibbs et al. (2001): NAR</b>	-----	<b>298.7 m/s</b>	-----	<b>D</b>
This study, 140	661 m	401 m/s	34.25%	C
This study, 141	442 m	338 m/s	13.15%	D
This study, 142	955 m	424 m/s	41.95%	C
<b>Gibbs et al. (2001): OLV</b>	-----	<b>544.7 m/s</b>	-----	<b>C</b>
This study, 121	870 m	580 m/s	6.48%	C
This study, 122	673 m	538 m/s	-1.23%	C
This study, 123	997 m	498 m/s	-8.57%	C
<b>Wills and Silva (1998): Lakeview School</b>	-----	<b>339.06 m/s</b>	-----	<b>D</b>
This study, 158	939 m	317 m/s	-6.51%	D
This study, 159	973 m	306 m/s	-9.75%	D
<b>ROSRINE Pico Rivera 2</b>	-----	<b>241.54 m/s</b>	-----	<b>D</b>
This study, 153	492 m	425 m/s	75.95%	C
This study, 154	221 m	381 m/s	57.74%	C
This study, 155	775 m	337 m/s	39.52%	D
<b>ROSRINE Downey South</b>	-----	<b>245.88 m/s</b>	-----	<b>D</b>
This study, 164	2412 m	326 m/s	32.59%	D

**Table 4**

Table 1: Velocity-profile modeling error tests at three randomly selected sites along the length of our transect. The first velocity of the second column ( $V_s^{30}$  Values) is the original analyst's result; the second velocity is the reanalyzed value.

Table 2: Key for Quaternary geological map units designated in Figure 4.

Table 3: Key for soil map units numbered in Figure 5.

Table 4: A comparison of borehole measurements within 1 km of our transect to our ReMi measurements. The downhole and suspension-logger results appear in a community data set assembled by Wills and Silva (1998), and including Gibbs et al. (2000), Gibbs et al. (2001), with further updates to April 2005 (C. Wills, pers. comm., 2005). See Fig. 3 for graphical plot of  $V_s^{30}$  values.

Figure 1: Location map of the transect area. The double line trending north-south locates our shallow shear-velocity transect. The site conditions map published by Wills et al. (2000) is included in the background. Letter labels are their hazard classification labels, meant to be similar to the NEHRP classification.

Figure 2: Gridded shear velocities for the entire transect in section to 200 m depth. Zero kilometers transect distance is the mouth of San Gabriel Canyon, and 60 km is at Seal Beach (Fig. 1). Velocity values related to NEHRP classification boundaries are provided. At each surface location, only the velocities above the 30-meter-depth line figure into calculating  $V_s^{30}$  values for Figure 3.

Figure 3:  $V_s^{30}$  values for 199 transect array measurements are shown as dark circles outlined with white. Corroborating lateral measurements away from the San Gabriel River are also shown with various symbols projected back upon the transect line. All values are positioned by the transect distance of the midpoint of the array from the mouth of San Gabriel Canyon. For comparison, hazard-classification velocity ranges from the study by Wills et al. (2000) are shown in light gray. Borehole measurements within 1 km of our transect are also included with various symbols from Table 4.

Figure 4: Measured  $V_s^{30}$  values compared to their respective geologic unit (CDMG, 1998). Dark diamonds represent the mean values and bars represent the standard deviation of the measurements. The x-axis is an approximate age scale with the oldest units to the left and the youngest units to the right. Average velocity and standard deviation values are shown for each unit. Populations are also shown. A key of geologic units can be found in Table 2, by label.

Figure 5: Measured  $V_s^{30}$  values compared to their respective soil unit (NRCS, 1969). Black diamonds represent the mean values and bars represent the standard deviation of the measurements. Average velocity and standard deviation values are shown for each unit. Populations are also shown. Consult Table 3 for a description of soil units, by number.

Figure 6: Correlation of our  $V_s^{30}$  measurements against the velocity ranges predicted by the classification map of Wills et al. (2000). Our transect observes good correlations for classes BC, D, and DE. Our ~30 class CD sites show an average above the expected range.

Figure 7: Variance versus distance to 50 km for our ReMi measurement data set (A); and for the community borehole data set inside the Los Angeles Basin (B) from Wills and Silva (1998), Gibbs et al. (2000; 2001), and updated to April 2005 (C. Wills, pers. comm., 2005). Here we plot as a circle the natural logarithm of the ratios of each  $V_s^{30}$  value against every other  $V_s^{30}$  value as a proxy for variance. Note in the expanded plots from 0-5 km distance (C and D) that variance is present even at very small distances. A and B have different vertical scales while C and D have the same scales. The borehole data set (D) shows finite variance at zero distance, from multiple measurements in boreholes at UCLA, Wilshire Blvd., and Whittier Narrows.

Figure 8: Comparison of ROSRINE/USGS Pico Rivera #2 suspension-logger results from [geoinfo.usc.edu/rosrine](http://geoinfo.usc.edu/rosrine) against three nearby ReMi arrays along our July 2003 transect. Below 8 m depth, velocities and interface depths match well. The ReMi arrays were all on the engineered riverside levee, and show

minimum shallow velocities greater than 200 m/s. The ROSRINE hole is only 221 m away from our transect, across the river channel, but has slow 100-200 m/s deposits in the upper 8 m, probably partly saturated clays.

Figure 9:  $V_s^{30}$  as a function of river gradient. Note the positive correlation of increasing  $V_s^{30}$  values with increasing gradient, most clear as a predictor of minimum  $V_s^{30}$  (light gray line).

Figure 10: Spatial power spectrum of our transect  $V_s^{30}$  values as a log-log plot. The power spectrum is the gray line and the trend line used to calculate the fractal dimension  $D$  of 1.70 is shown in black. The computed fractal dimension changes to 1.78 if the noise floor of the spectrum at <700 m spacing is omitted from the regression.

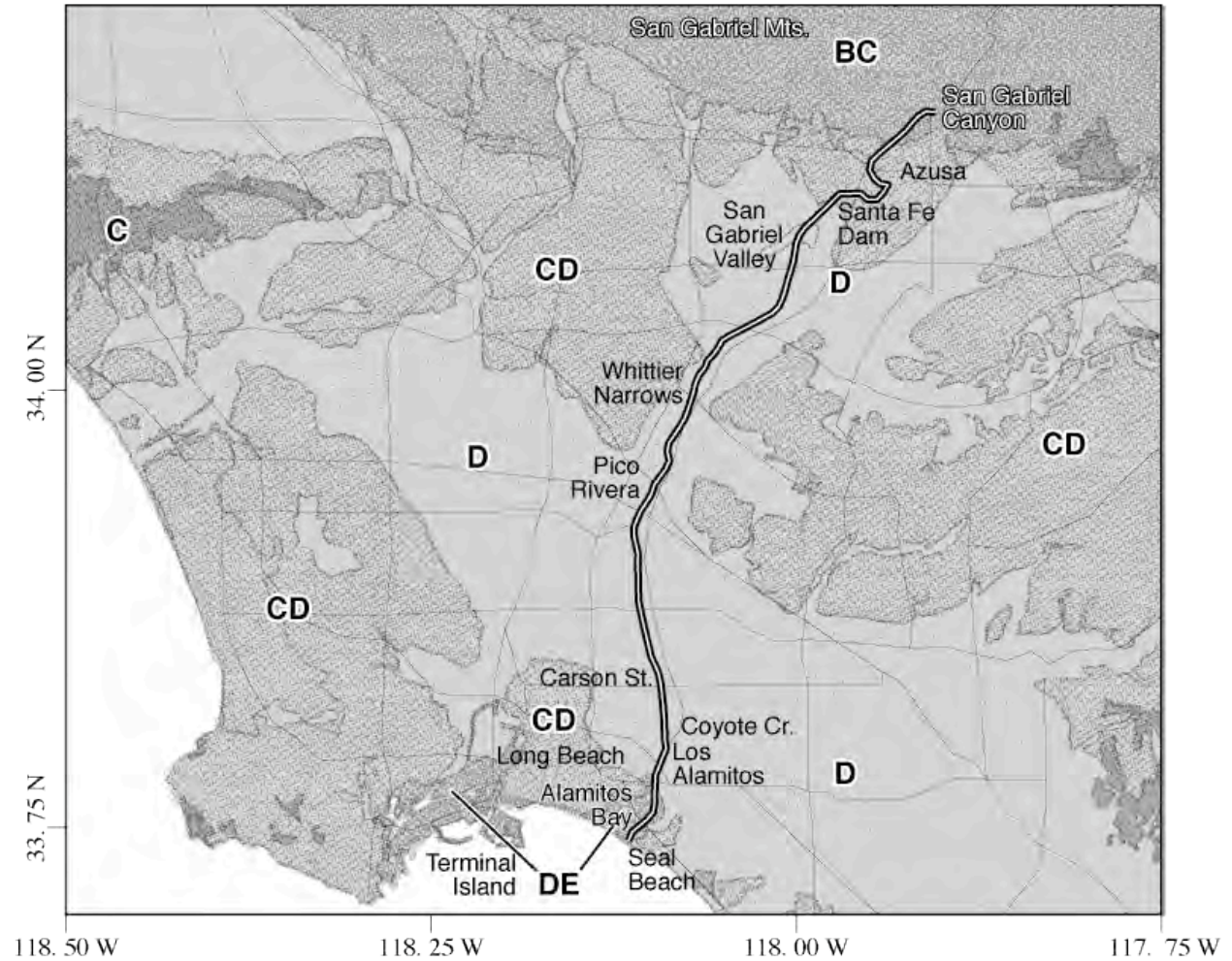


Figure 1

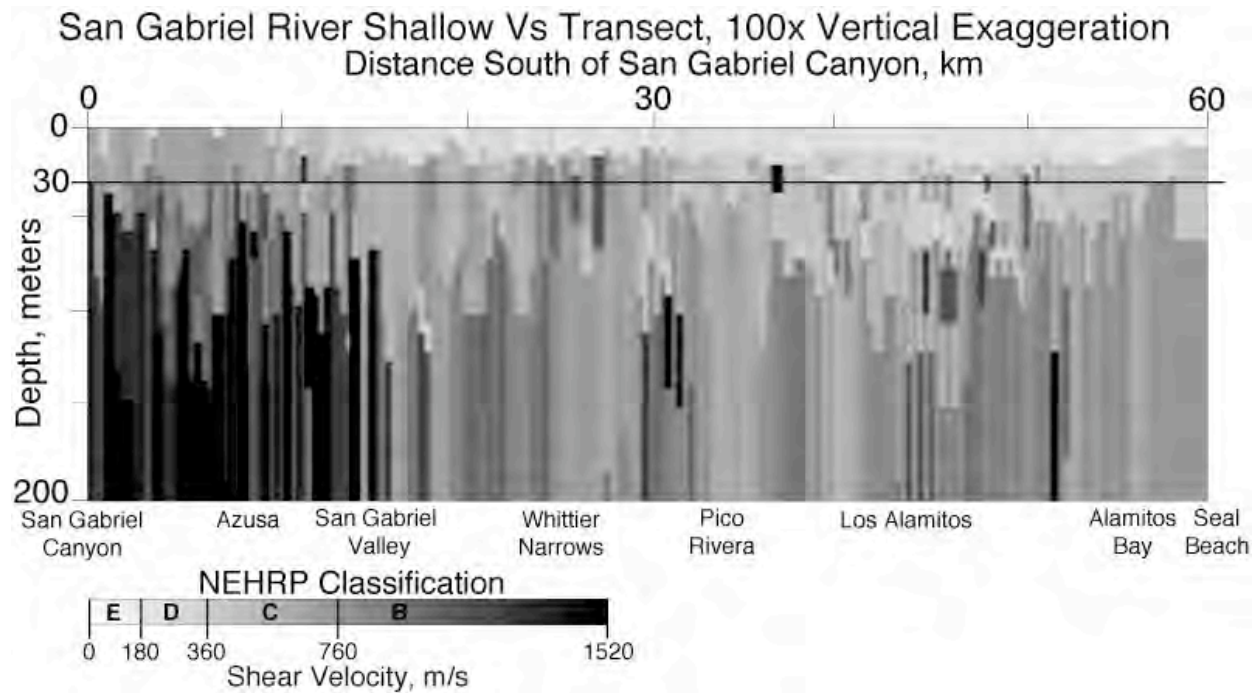


Figure 2

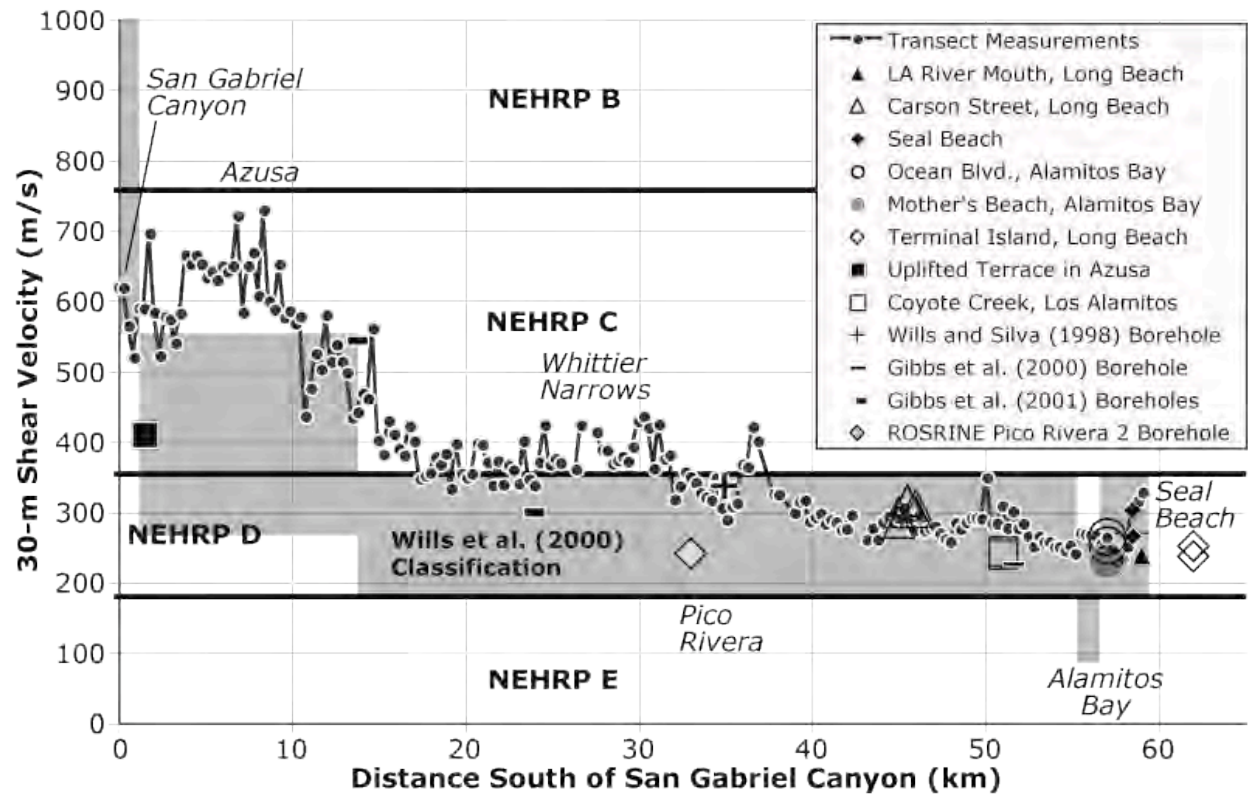


Figure 3

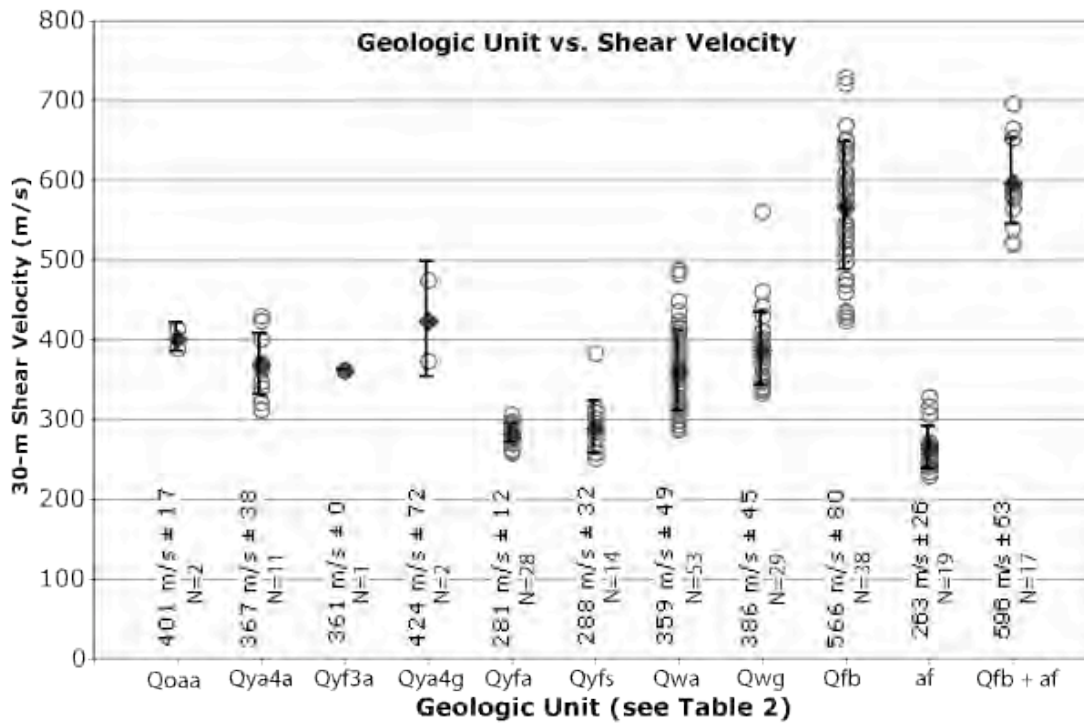


Figure 4

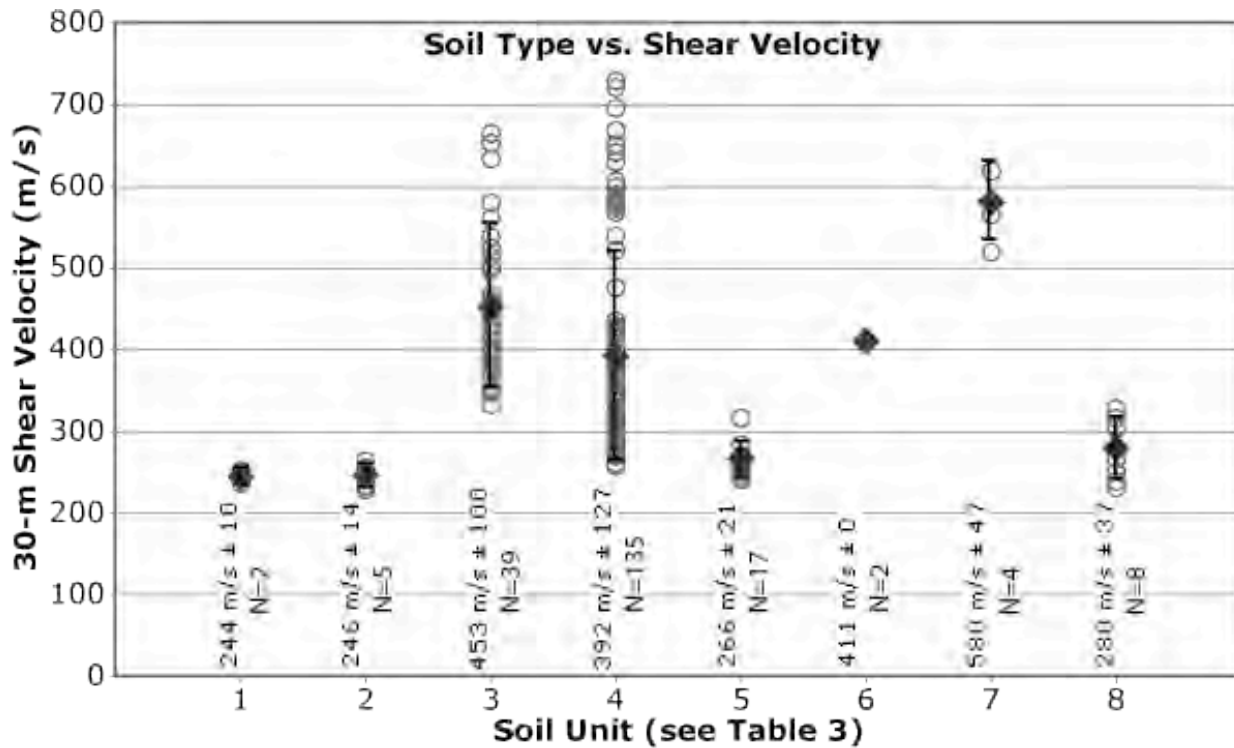


Figure 5

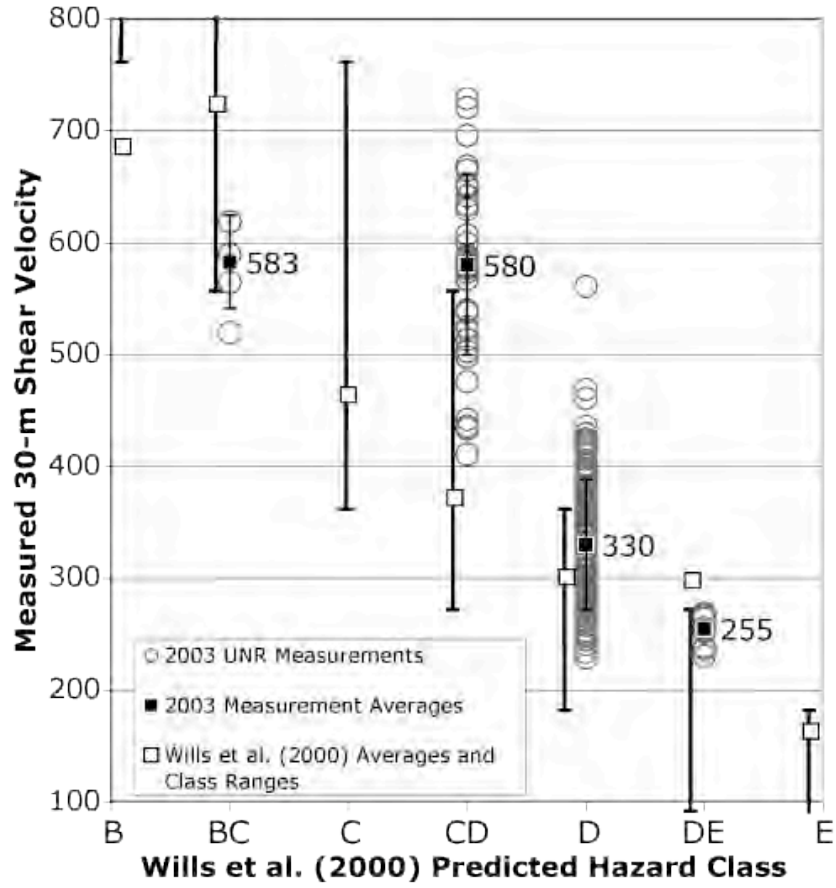


Figure 6

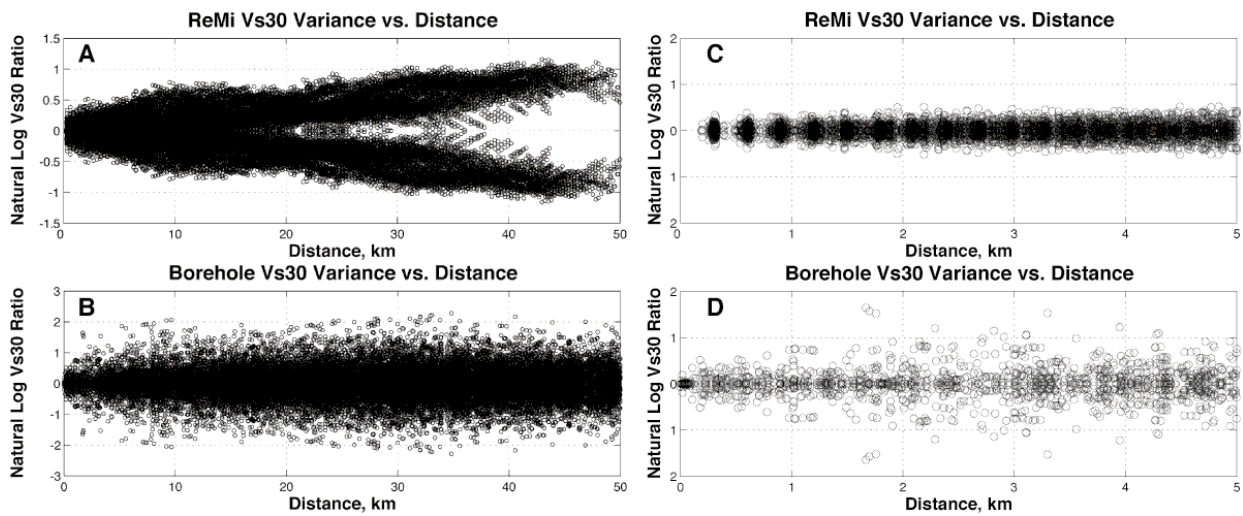


Figure 7

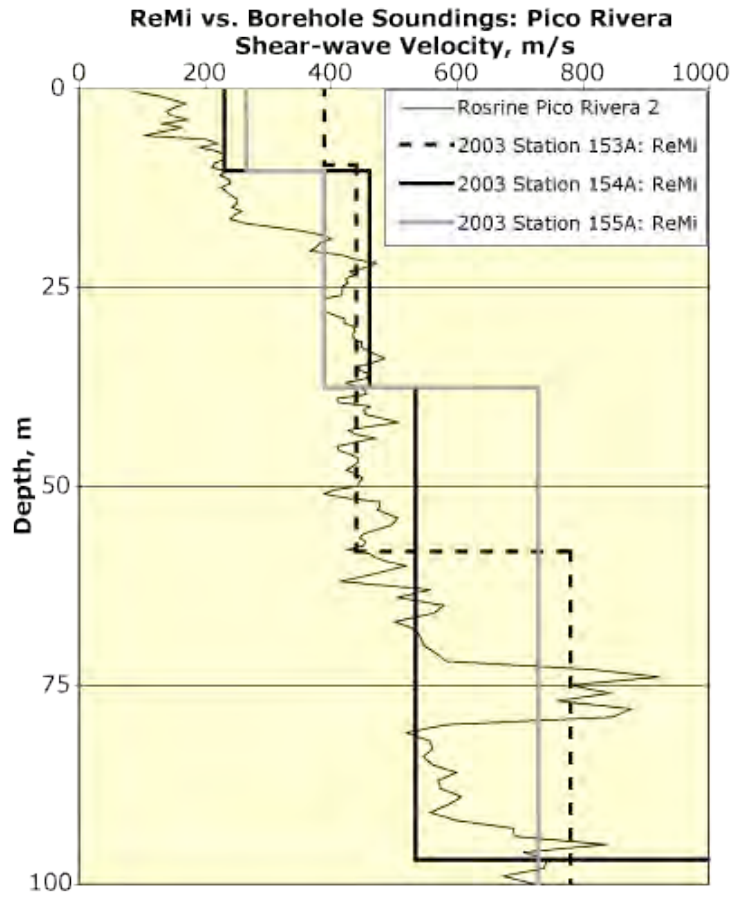


Figure 8

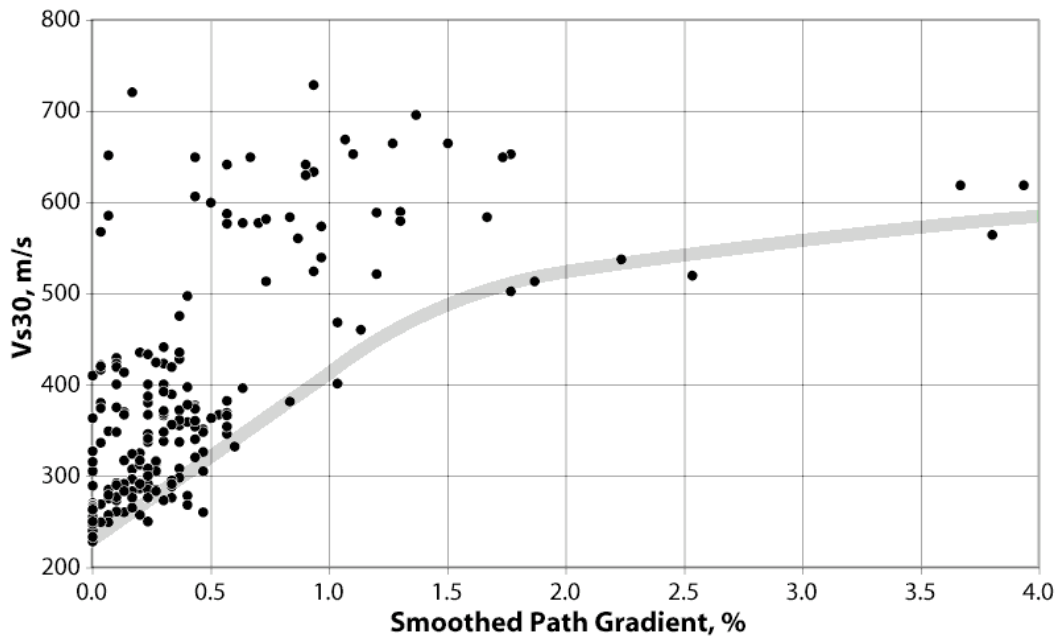


Figure 9

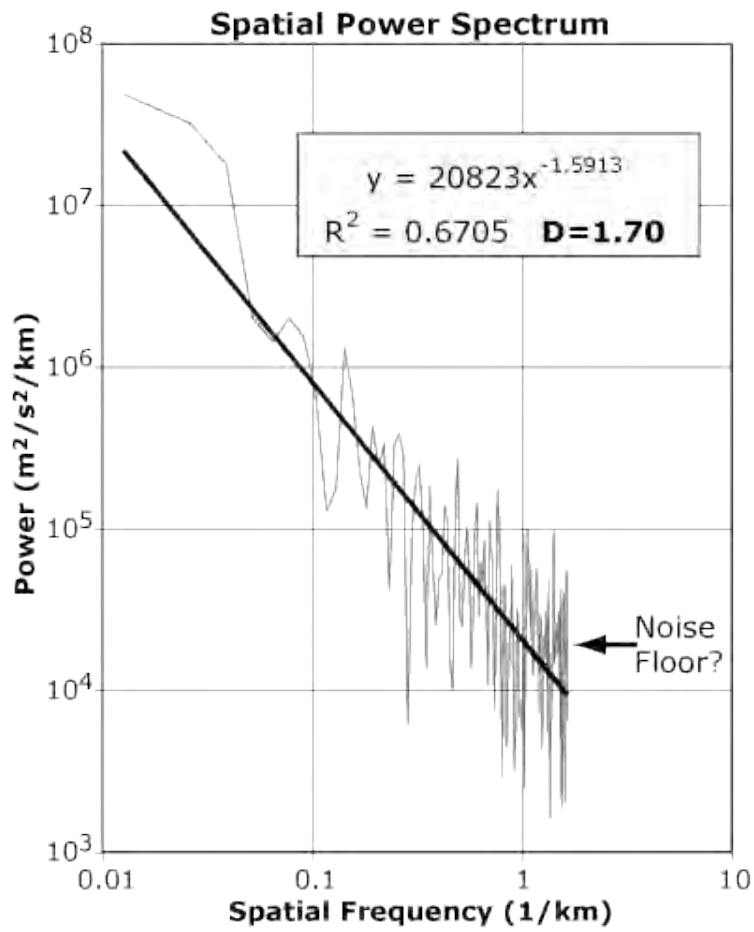


Figure 10